

Slow dynamics in many-body localized system with random and quasi-periodic potential

Felix Weiner,¹ Ferdinand Evers,¹ and Soumya Bera²

¹*Institute of Theoretical Physics, University of Regensburg, D-93040 Germany*

²*Department of Physics, Indian Institute of Technology Bombay, Mumbai 400076, India*

(Dated: July 3, 2022)

We investigate charge relaxation in disordered and quasi-periodic quantum-wires of spin-less fermions (t - V -model) at different inhomogeneity strength W in the localized and nearly-localized regime. Our observable is the time-dependent density correlation function, $\Phi(x, t)$, at infinite temperature. We find that disordered and quasi-periodic models behave qualitatively similar: Although even at longest observation times the width $\Delta x(t)$ of $\Phi(x, t)$ does not exceed significantly the non-interacting localization length, ξ_0 , however strong finite-size effects are encountered. We conclude that rare disorder configurations (Griffiths effects) are not a likely cause for the slow dynamics observed by us and earlier computational studies. As a relatively reliable indicator for the boundary towards the many-body localized (MBL) regime even under these conditions, we consider the exponent function $\beta(t) = d \ln \Delta x(t) / d \ln t$. Motivated by our numerical data for β , we discuss a scenario in which the MBL-phase splits into two subphases: in MBL_A $\Delta x(t)$ diverges slower than any power, while it converges towards a finite value in MBL_B . Within the scenario the transition between MBL_A and the ergodic phase is characterized by a length scale, ξ , that exhibits an essential singularity $\ln \xi \sim 1/|W - W_{c1}|$. Relations to earlier proposals of two-phase scenarios will be discussed.

Introduction. The interplay of quantum interference and interactions exhibits some of the most fascinating phenomena to be encountered in many-body systems. A typical representative of concern to us here is *many-body localization*^{1,2} (MBL), which has attracted considerable attention over the last decade^{3–12}. At its heart is the basic observation that Anderson localization prevalent in low-dimensional, disordered systems of non-interacting fermions can be robust against interaction effects at finite temperature despite of dephasing.

Starting from the MBL phase with decreasing disorder a quantum-critical point is reached separating the MBL region from an ergodic one. Much progress has been made in recent years with respect to experimental investigations of the corresponding localization-delocalization transition in diverse setups including cold atoms^{13–18}, nuclear spin chains¹⁹, Yb ion system²⁰, dipolar spins²¹, or in InO thin films²². Importantly, in several experiments a very pronounced slow-down of the relaxation dynamics has been reported, when the (quasi-)disorder strength exceeds a threshold value^{15,16,18}.

The theoretical investigation of MBL and the related effects poses great challenges. On the one hand side the phenomenon escapes controlled analytical investigations. On the other hand, the computationally available window of observation times, t_{obs} , and system sizes often is too small in order to predict with confidence the thermodynamic, long time asymptotics. In fact as shown recently, due to dynamical slowing down, even in computational studies of the ergodic regime the width of the diffusion propagator, $\Delta x(t)$, is hardly ever seen to exceed the non-interacting localization length, ξ_0 , significantly²³. The resulting difficulties to safely extrapolate plague virtually all computational studies of dynamical behavior near and in the MBL phase.²⁴ In fact, even present days experimental studies do not (yet) allow to

go very deeply into the asymptotic regime. Summarizing, a possibility to get stuck with transient behavior has to be accounted for. Nevertheless from combining computational studies employing a variety of numerical techniques and analytical arguments based, e.g., on phenomenological renormalization-group treatments, a certain picture has emerged. It has been surveyed in several recent reviews^{11,12,25–29}.

In this work we present a computational study of the MBL region employing the t - V -model with fully random and quasi-periodic (Andre-Aubry-type) potentials^{30–34}.

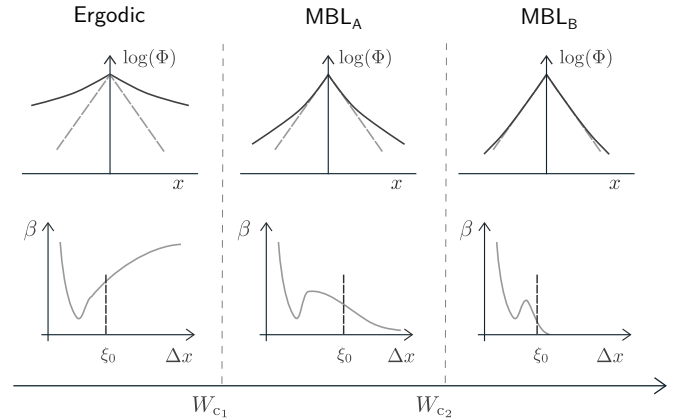


FIG. 1. Proposed infinite temperature phase diagram of the t - V -model indicating the possible splitting of the MBL-phase into subphases. Upper panel: schematic behavior of density-density correlation function $\Phi(x, t)$. Lower panel: corresponding effective exponent β (defined in Eq. (1)) plotted over the variance of $\Phi(x, t)$, which is $\Delta x(t)$; ξ_0 indicates the non-interacting localization length. Between ergodic phase and MBL_A , $\beta(x \approx \xi_0)$ changes sign; once MBL_B is reached, β vanishes at a finite Δx .

We invoke as observable the density-density correlation function, $\Phi(x, t)$. The growths of its variance in time, $\Delta x(t)$, defines the exponent function

$$\beta(t) = \frac{d \ln \Delta x(t)}{d \ln t}. \quad (1)$$

Previous authors have exploited its long time limit, $\beta_\infty(W) \equiv \beta(t \rightarrow \infty)$, or closely related exponents as an effective “order parameter”; in the ergodic region prevailing at disorder $W < W_c$ one has $\beta_\infty > 0$, while the MBL-phase, $W > W_c$, has been defined by $\beta_\infty = 0$.³⁵ However, the data we here report leaves open a possibility for an intermediate window, $W_{c1} < W < W_{c2}$, which constitutes within the MBL-phase a subphase MBL_A; It exhibits a width $\Delta x(t)$ diverging in time but with a growth weaker than any power, see Fig. 1 for a sketch and Fig. 2 for illustrating data. At very large disorder, $W > W_{c2}$, one enters the subphase, MBL_B, in which $\beta(t) \rightarrow 0$ upon $\Delta x(t)$ approaching the localization length $\xi(W)$.

In view of the difficulty accessing the asymptotic regime of $\beta(t)$, we consider as a pragmatic indicator in addition to β also its slope, $\dot{\beta}$, taken at the computationally still accessible (i.e. relatively short) times t_ξ , where $\Delta x(t)$ has passed the largest relevant microscopic length.³⁶ Following this idea, entering the MBL_A-phase from the ergodic side at $W = W_{c1}$ is signaled by a change of sign in $\dot{\beta}(t)$ at $t \gtrsim t_\xi$. While the ergodic phase is char-

acterized by $\beta(t) > 0, \dot{\beta}(t) > 0$, we have $\beta(t) > 0, \dot{\beta}(t) < 0$ in MBL_A. A natural candidate for the microscopic length appearing in t_ξ is the localization length, $\xi_0(W)$, of the non-interacting reference system, possibly having undergone an interaction-mediated (static) renormalization. Hence, we define t_ξ implicitly via

$$\Delta x(t_\xi) \approx \xi_0. \quad (2)$$

We list the salient aspects of our numerics and the scenario displayed schematically in Fig. 1: (i) In the ergodic phase, $\Delta x(t) \sim t^\beta$, where $\beta(t)$ converges to a constant with $\dot{\beta}(t)$ approaching zero from above; correspondingly, the slope $\dot{\beta}(t_\xi)$ seen in the numerical data should be positive when converged with respect to computational parameters. In MBL_A the asymptotic growth of $\Delta x(t)$ is also unbound, but $\beta(t) \rightarrow 0$ with $\dot{\beta}(t)$ approaching zero from below; correspondingly, $\dot{\beta}(t_\xi)$ seen in the numerical data is negative when converged. Finally, in MBL_B $\Delta x(t)$ is bounded from above and β extrapolates to zero at a finite Δx . We interpret the numerical data shown in Fig. 3 as reflecting the evolution with increasing disorder strength W described here and in Fig. 1. The existence of an intermediate phase has been proposed before³⁷; the relation to our scenario is discussed below.

(ii) We have applied our analysis method to the t - V model with fully disordered and quasi-periodic potential. Importantly, comparing both cases we cannot detect an essential difference in the evolution of $\Delta x(t)$ with the inhomogeneity strength. Therefore, our results seem hard to reconcile with Griffiths-type scenarios that rely on rare-regions to explain the origin of slow dynamics^{27,28,38}.

(iii) To formulate our scenario we adopt the spirit of mode-coupling theory extrapolating into the asymptotic regime.

It suggests that the localization length ξ , when entering MBL_A from the ergodic phase, exhibits an essential singularity rather than a power-law, which is consistent with the Harris-Chayes criterion³⁹.

Model system and computational method. We consider the t - V -model

$$\hat{\mathcal{H}} = -\frac{t_h}{2} \sum_{x=1}^{L-1} \hat{c}_x^\dagger \hat{c}_{x+1} + h.c. + \sum_{x=1}^L \epsilon_x \left(\hat{n}_x - \frac{1}{2} \right) + V \sum_{x=1}^{L-1} \left(\hat{n}_x - \frac{1}{2} \right) \left(\hat{n}_{x+1} - \frac{1}{2} \right), \quad (3)$$

where hopping is over L sites with amplitude t_h . We work at a half filling and with hard-wall boundary conditions. When employing disordered potentials, the onsite-energies, ϵ_x , are drawn from a box distribution $[-W, W]$.⁴⁰ In subsequent calculations the interactions taken twice larger, $V = 2t_h$, than in previous studies²³ to emphasize interaction effects. At the disorder values shown in Fig. 2, the spectral statistics is close to Poissonian and in this sense the system is many-body localized, see supplemental information A.

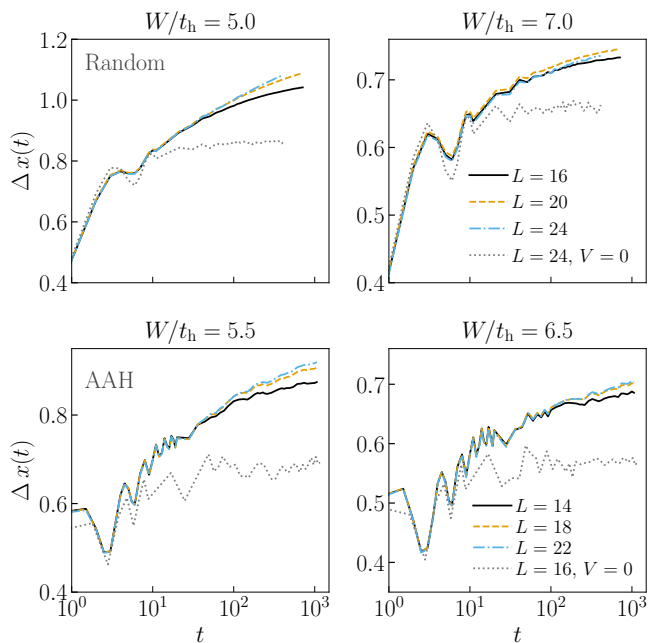


FIG. 2. Time evolution of $\Delta x(t)$ with disordered (random, upper row) and quasi-periodic (lower row) potential in MBL_A (left) and closer to MBL_B (right) phases as obtained in t - V model. In MBL_A a very slow growth (“creep”) is observed in both potential-types that stabilizes with increasing system size. (Simulation parameters: $V/t_h = 2.0$; $W/t_h = \{5.0, 7.0\}$ (random) and $W/t_h = \{5.5, 6.5\}$ (quasi-periodic).)

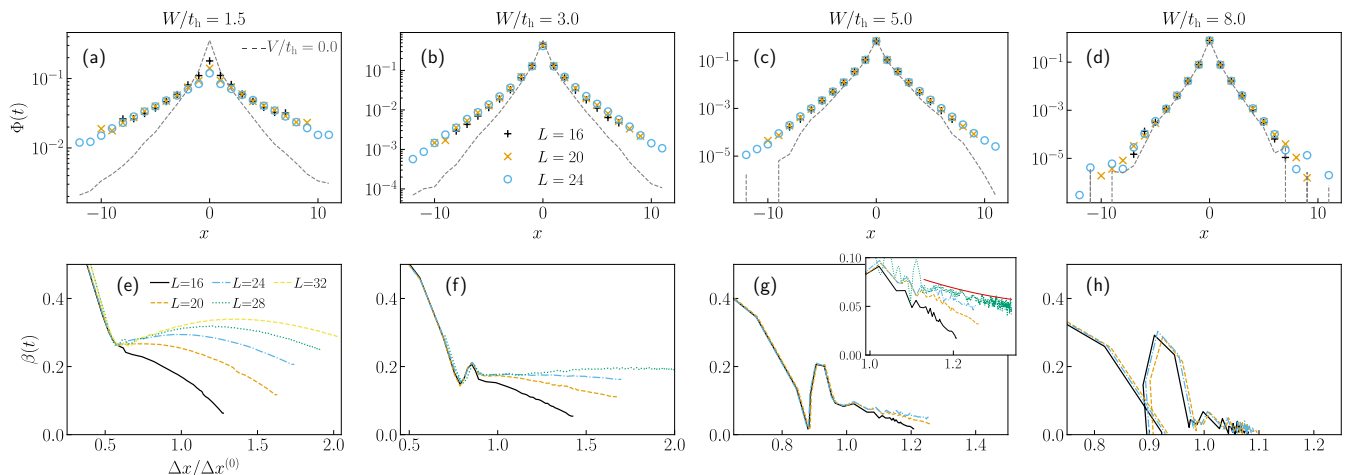


FIG. 3. Effect of interactions with increasing disorder monitored by the density-density correlation function $\Phi(x, t)$; the analogous plot for the quasi-periodic model is shown in supplemental information D. Upper row: $\Phi(x, t)$ for system sizes $L=16, 20, 24$ and disorder $W=1.5, 3.0, 5.0, 8.0$ at $t \approx 400t_h^{-1}$. The non-interacting result at $L=24$ is also shown for reference (dashed line). The plot highlights how creep begins to manifest at larger disorder by “lifting the tails” of $\Phi(x, t)$. Lower row: The exponent function $\beta(t)$ corresponding to first-row data plotted over $\Delta x(t)/\Delta x^{(0)}$ as suggested by Eq. (5); $\Delta x^{(0)}$ denotes the saturation width of the non-interacting diffusion propagator at long time, here taken as an indicator of ξ_0 . β inherits finite-size corrections from $\Phi(x, t)$, which persists also at larger disorder values as is seen, e.g., in the inset. The red line in there serves as guide to the eye. The evolution seen in this data condenses into the schematics displayed in Fig. 1. The noise visible at larger W -values reflects statistical noise from disorder averaging. The average was taken over ~ 10000 samples for largest system size and for largest disorder values, while for smaller system sizes ($L = 16, 20$) the disorder averaging is performed over ~ 20000 samples.

Our observable is the density-density correlator,

$$\overline{\Phi(x, t)} = \overline{\langle (\hat{n}_x(t) - \frac{1}{2})(\hat{n}_0 - \frac{1}{2}) \rangle \Theta(t)}, \quad (4)$$

with primary focus on the second moment,

$$\Delta x(t) = \left[\overline{\sum_{x=-L/2}^{L/2} x^2 \Phi(x, t) - \left(\sum_{x=-L/2}^{L/2} x \Phi(x, t) \right)^2} \right]^{1/2}.$$

The disorder average is indicated by an overline; the thermal average is performed at infinite temperature and denoted by angular brackets, $\langle \dots \rangle$; corresponding traces are performed stochastically.⁴¹ For the time evolution, Eq. (4), we employ a standard Chebyshev-polynomial propagation⁴²; further details are given in Ref. 23.

Computational results. We systematically analyze traces of the kind shown in Fig. 2 in terms of the logarithmic derivative (1); the results are shown in Fig. 3. The top-row displays the evolution of $\Phi(x, t)$ with system size and disorder at $t: = t_{\text{obs}} \sim 400t_h^{-1}$. Fully consistent with our earlier findings, $\Phi(x, t)$ exhibits a pronounced non-Gaussian, nearly exponential shape – here seen in a wide range of W -values. Not surprisingly, the interaction effects on $\Phi(x, t)$ are strongest in the tails; they emerge gradually, with ever increasing system size L and observation time. Note that at larger disorder the interacting and non-interacting traces are seen to almost coincide for smaller distances at the time observed, see,

e.g., Fig. 3, $W > 5$. At these (possibly transient) times one has $\Delta x(t) \approx \Delta x^{(0)}$. Therefore, interaction-related static renormalization effects of the disorder-strength are small at $W \gtrsim V$.

The lower row of Fig. 3 is the basis of the schematic plot Fig. 1. It shows the exponent function $\beta(t)$ that highlights the important effects related to finite L . Consistent with our previous findings²³, at weak disorder $W \lesssim 3$ and $\Delta x(t) \sim \Delta x_0$ there is a system size convergence with respect to the sign of the slope of $\beta(t)$; there is no notion of convergence at $\Delta x(t) \gtrsim \Delta x_0$ beyond the statement that $\beta(\Delta x)$ is curved to the right. At larger disorder, $W \gtrsim 5$, a qualitative change is observed: the curvature seen in the inset of Fig. 3 is about to turn left at $\Delta x(t) > \Delta x_0$. The MBL_A scenario advocated in Fig. 1 is based on the observation that the curvature of $\beta(\Delta x)$ changes sign with growing W together with the assumption that there is no turn-around in $\beta(\Delta x)$ to follow, but rather a smooth decay towards the horizontal axis at $\Delta x \rightarrow \infty$. (A discussion of the pronounced short-time feature of the data Fig. 3 lower row, namely the spike growing in $\beta(\Delta x)$ with increasing W near Δx_0 , is given in the supplemental information C.)

Phenomenological modeling. The data for the β -function displayed in Fig. 3 condenses into the phenomenological ansatz

$$\beta[\Delta x] = \frac{b}{1 + b_1 \mathcal{K}(\xi_0/\Delta x)}. \quad (5)$$

Similar to our previous work²³, we here consider β as a functional of the slowest dynamical mode, which for simplicity we parametrize with $\Delta x(t)$; the parameters b, b_1 and the kernel \mathcal{K} are evolving with disorder W . The ansatz helps formulating a scenario for the qualitative properties of the long-time limit, which are just barely seen to emerge in Fig. 3.

Embarking on (5) we describe a passage from the ergodic regime through MBL_A into MBL_B with increasing W . The kernel $\mathcal{K}(y)$ equals unity at $y=1$ and otherwise is assumed to be a monotonous function in the interval $1 \gtrsim y \gtrsim 0$. Its precise form is evolving with the disorder strength, W : With decreasing y , the kernel decreases in the ergodic phase, increases in MBL_A and is seen to diverge at a finite y upon entering MBL_B .

Ergodic regime $W < W_{c_1}$. The power-law growth of $\Delta x(t)$ characteristic for the ergodic regime is captured by (5) with $b > 0, b_1 > 0$ and taking $\mathcal{K}(y)$ as decreasing to zero in the limit $y \rightarrow 0$. Namely, with the variance $\Delta x(t)$ growing in time, the kernel $\mathcal{K}(\xi_0/\Delta x(t))$ vanishes and so the denominator converges to unity. At this point, b should be identified with the diffusion exponent: $b = \beta_\infty$

Transition into MBL_A . The transition is associated with a vanishing slope, $\beta=0$. Within in the setting (5) this requires the existence of a particular value of the disorder W_{c_1} , such that the contribution of the term containing $b_1 \mathcal{K}(\lambda/\Delta x)$ is independent of Δx . This situation could be realized in several ways; the most plausible scenario is $\mathcal{K}(y)|_{W_{c_1}} = 1$.⁴³ We thus parameterize $\mathcal{K}(y)$ in the vicinity of $W \approx W_{c_1}$ as follows:

$$\mathcal{K}(y) \approx \tilde{\mathcal{K}}(y)^{W-W_{c_1}}, \quad \tilde{\mathcal{K}}(y) := e^{\frac{d \ln \mathcal{K}(y)}{dW}}|_{W_{c_1}}. \quad (6)$$

This shape has consequences for the localization lengths,

$$1 \approx b_1 \mathcal{K}(\xi_0/\xi). \quad (7)$$

which we here define implicitly; we have

$$\tilde{\mathcal{K}}(\xi_0/\xi) \approx b_1^{\frac{1}{(W_{c_1}-W)}}. \quad (8)$$

To illustrate the impact of this statement, we adopt a power-law shape $\tilde{\mathcal{K}}(\xi_0/\xi) \sim (\xi/\xi_0)^\kappa$, $\kappa > 0$, so that

$$\xi \sim \xi_0 b_1^{\frac{1}{\kappa(W_{c_1}-W)}}. \quad (9)$$

It is thus seen that the scenario formulated in (5) tends to generate length scales that are diverging at the transition in an exponential rather than in a power-law fashion.

MBL_A -phase. According to (6), in MBL_A the kernel $\mathcal{K}(y)$ diverges with $y \rightarrow 0$ keeping $b > 0$ and $b_1 > 0$. With growing time, the second term in the denominator grows without bound and eventually

$$\beta(\Delta x) \approx \frac{b}{b_1} \mathcal{K}(\xi_0/\Delta x)^{-1}.$$

The behavior is consistent with the data Fig. 3 as seen, e.g., at $W=5$. It predicts for the β -function a decay approaching zero upon $\Delta x(t) \rightarrow \infty$.

Transition into the MBL_B -phase. Upon approaching W_{c_2} and MBL_B the kernel $\mathcal{K}(y)$ diverges at a nonvanishing value y_c . For illustration we adopt the generic form

$$\mathcal{K}(y) = \frac{y^\alpha}{1 + b_2 y^{1/\nu}} \quad (10)$$

with $\alpha, \nu > 0$. In MBL_A , we have $b_2 > 0$ and so the kernel diverges in a power-law fashion, $\mathcal{K}(y) \sim y^{\alpha-1/\nu}$, as required. When W crosses W_{c_2} from below, the coefficient $b_2(W)$ changes sign from positive to negative, so in MBL_B the kernel diverges at $y^{1/\nu} = |b_2|^{-1}$. We conclude that the localization length diverges $\xi \approx \lambda |W_{c_2} - W|^{-\nu}$.

Discussion. The model (5) has implications, which can be tested further. We mention the following two: (i) When entering MBL_A from the ergodic side, $\beta_\infty(W_{c_1})$ is taking a non-vanishing, critical value. In contrast, at the critical point separating MBL_B and MBL_A $\beta_\infty(W_{c_2})=0$ is expected. (ii) Previous computational studies have attempted a scaling analysis near $W \approx W_{c_1}$ in order to extract a localization length exponent based on a power-law dependency $\xi \sim |W - W_{c_1}|^{-\nu}$. The value of ν has not consolidated, yet: Luitz et al.⁸ obtained $\nu \approx 0.7$ from the system size scaling of the magnetization density, violating the Harris-Chayes bound $\nu > 1$ in one dimension³⁹. This led to a subsequent discussion⁴⁴ attempting at rationalizing this result. On the other hand, recent exact diagonalization studies of the scaling of the Schmidt gap⁴⁵ or local temperature fluctuations⁴⁶ found exponents exceeding 2 consistent with the Harris bound. We point out that within the scenario here lined out the transition that has been investigated in these studies would correspond to the entry into MBL_A , so the localization length diverges stronger than any power. Hence, the Harris-Chayes bound is satisfied automatically.

Saying this we emphasize once again the exploratory character of the scenario developed with Eq. (5). Due to creep, we do not see at present a reliable way of telling, whether the system actually localizes, i.e., if W_{c_2} is finite or not. We stress that creep is a phenomenon that gradually emerges at largest system sizes, longest time scales and only in the tails of the distribution (3). For observing or ruling out creep with frequently employed observables, such as the level statistics, the return probability or the sublattice imbalance, deviations have to be identified from the non-interacting background-behavior; such deviations manifest as small signals towards delocalization that slowly grow with increasing time and system size and thus are challenging to consolidate.

Relation to RG-studies. We compare our scenario with recent renormalization group (RG) calculations^{37,47-49} and a numerical study⁵⁰. Reference 37 predicts an intermediate MBL phase; also in this case the typical localization length diverges exponentially (implying $\nu=\infty$) near the ergodic transition, however with an exponent $|W - W_{c_1}|^{-1/2}$ (rather than $|W - W_{c_1}|^{-1}$). This intermediate phase is distinguished by having power-law distributed rare thermal blocks with an exponent taking a universal value at the critical point^{37,47,50}; at strong

disorder the distribution becomes exponential. A picture invoking rare thermal blocks, i.e. a Griffith region within the MBL phase, has already been proposed in earlier phenomenological renormalization group settings^{48,49}.

In order to clarify if creep relates to rare disorder fluctuations, we have been comparing dynamics in random and quasi-periodic potentials in Fig. 2, see also supplemental information C. Remarkably, we observe a qualitatively similar slow dynamics in both cases. Therefore, it seems unlikely that rare events can explain creep as observed, e.g., in Fig. 3.

Our assertion of slow dynamics receives (tentative) support from most recent experiments in optical lattices¹⁸. The Bose-Hubbard model was simulated with quasi-periodic disorder potential; a slow particle transport has been seen at finite system sizes ($L = 8, 12$) above the critical disorder strength. We would like to interpret this observation as a possible experimental manifestation of a creep-type dynamics.

Relation to earlier numerical studies. Recently, Gopalakrishnan et. al.⁵¹ reported a low-frequency asymptotics of the conductivity $\sigma(\omega) \sim |\omega|^\alpha$ with an exponent α varying continuously within a region in the MBL-phase. At stronger disorder the agreement reflects the fact that interaction effects are almost invisible in the numerical data, so the non-interacting result $\alpha \sim 2$ is reached trivially at large W within the available range of computational parameters. At weaker disorder near the border to the thermal phase, Gopalakrishnan et al.⁵¹ give a smaller value $\alpha \sim 1$ corresponding to a logarithmic growth of $\Delta x(t)$. This is consistent with the behavior we observe in MBL_A (see Fig. 2). In fact, a more recent study⁵² on significantly larger system sizes reports $\alpha \sim 1$ in a broad window of disorder strengths near the transition. We mention, however, that an exponent varying continuously across the transition, $\alpha(W)$, has also been found in a self-consistent perturbation theory in disorder⁵³.

Similarly, also Barišić et. al.⁵⁴ report values $\alpha \sim 1$ in the MBL-phase, employing system sizes up to $L=28$. In their fitting, the authors are allowing for a non-vanishing residual dc-conductivity, however, and indicate that finite size corrections are not fully under control. So, we understand that the numerical value $\alpha=1$ is subject to a significant uncertainty. The same group later extended their studies to related correlation functions^{29,55}. Reminiscent of creep, also in these correlators a very slow dynamics with significant finite-size effects can be identified, e.g., in Fig. 2 (c,d) of Mierzejewski et al.⁵⁵.

Finally, the sparsity of many-body states in Fock-space

can give rise to a kind of multifractality, which exhibits a non-universal and, in general, basis dependent spectrum^{56,57}. Most recent numerical work has confirmed this suspicion at least within a certain window of system sizes computationally available⁵⁸. Conceivably, multifractality of the many-body wavefunction manifests in the evolution of $\alpha(W)$.

Conclusion: In this work we have studied the density autocorrelation function of spinless fermions. We detect a very slow dynamics with a tendency towards delocalization even at strong disorder, where the level statistics is (at least very close to) Poissonian. Our results imply one out of two possibilities:

Either the critical disorder value exceeds all other relevant energy scales by far, $W_c \gg V, 4t_h$, and hence exceeds most current computational estimates significantly. In this case our simulations may be in the regime $W < W_c$ and we are observing an extremely slow thermalization process. The slow "creep" dynamics may indicate that the present understanding of the many-body localization is incomplete and might, e.g., overlook the existence of marginally thermalizing subphases, called MBL_A in this work. We propose that such phases can be described by complementing the concept of local integrals of motion^{59,60}, which has been developed for the case $W > W_c$, with a weak integrability breaking mechanism.

The alternative possibility is that simulations are actually in the proper MBL-regime, $W > W_c$, and we observe transient behavior, perhaps indicative of the critical fan⁴⁴ (similarly for quasi-periodic potential³³). Due to the extremely slow dynamics, the asymptotic regime is very difficult to reach in a controlled way, so the properties of the MBL-phase, e.g., the interacting localization length and its critical behavior are challenging to simulate.

Acknowledgement

We express our sincere gratitude to I. Gornyi, V. Khemani, J. Moore, A. Mirlin and D. Polyakov for inspiring discussion. SB would like to thank G. De Tomasi for earlier collaboration on a similar topic and for many insightful discussions. SB acknowledges support from DST, India, through Ramanujan Fellowship Grant No. SB/S2/RJN-128/2016 and ECR/2018/000876; FE was supported from the DFG under Grants No. EV30/11-1 and EV30/12-1. We acknowledge computing time on the supercomputer ForHLR funded by the Ministry of Science, Research and the Arts Baden-Württemberg and by the Federal Ministry of Education and Research.

¹ D. M. Basko, I. L. Aleiner, and B. L. Altshuler, *Ann. Phys.* **321**, 1126 (2006).

² I. V. Gornyi, A. D. Mirlin, and D. G. Polyakov, *Phys. Rev. Lett.* **95**, 206603 (2005).

³ M. Žnidarič, T. Prosen, and P. Prelovšek, *Phys. Rev. B* **77**, 064426 (2008).

⁴ A. Pal and D. A. Huse, *Phys. Rev. B* **82**, 174411 (2010).

⁵ J. H. Bardarson, F. Pollmann, and J. E. Moore, *Phys. Rev. Lett.* **109**, 017202 (2012).

- ⁶ R. Nandkishore and D. A. Huse, *Ann. Rev. Condens. Matter Phys.* **6**, 15 (2015).
- ⁷ E. Altman and R. Vosk, *Ann. Rev. Condens. Matter Phys.* **6**, 383 (2015).
- ⁸ D. J. Luitz, N. Laflorencie, and F. Alet, *Phys. Rev. B* **91**, 081103 (2015).
- ⁹ S. Bera, H. Schomerus, F. Heidrich-Meisner, and J. H. Bardarson, *Phys. Rev. Lett.* **115**, 046603 (2015).
- ¹⁰ Ann. Phys. (Berlin), in [Special Issue: Many-Body Localization](#), Vol. 529, edited by J. H. Bardarson, F. Pollmann, U. Schneider, and S. Sondhi (2017) p. 1770050.
- ¹¹ F. Alet and N. Laflorencie, *C. R. Phys.* (2018).
- ¹² D. A. Abanin, E. Altman, I. Bloch, and M. Serbyn, arXiv e-prints, arXiv:1804.11065 (2018), arXiv:1804.11065 [cond-mat.dis-nn].
- ¹³ M. Schreiber, S. S. Hodgman, P. Bordia, H. P. Lüschen, M. H. Fischer, R. Vosk, E. Altman, U. Schneider, and I. Bloch, *Science* **349**, 842 (2015).
- ¹⁴ J.-Y. Choi, S. Hild, J. Zeiher, P. Schauß, A. Rubio-Abadal, T. Yefsah, V. Khemani, D. A. Huse, I. Bloch, and C. Gross, *Science* **352**, 1547 (2016).
- ¹⁵ H. P. Lüschen, P. Bordia, S. Scherg, F. Alet, E. Altman, U. Schneider, and I. Bloch, *Phys. Rev. Lett.* **119**, 260401 (2017).
- ¹⁶ P. Bordia, H. Lüschen, S. Scherg, S. Gopalakrishnan, M. Knap, U. Schneider, and I. Bloch, *Phys. Rev. X* **7**, 041047 (2017).
- ¹⁷ T. Kohlert, S. Scherg, X. Li, H. P. Lüschen, S. Das Sarma, I. Bloch, and M. Aidelsburger, arXiv e-prints, arXiv:1809.04055 (2018), arXiv:1809.04055 [cond-mat.quant-gas].
- ¹⁸ M. Rispoli, A. Lukin, R. Schittko, S. Kim, M. E. Tai, J. Léonard, and M. Greiner, arXiv e-prints, arXiv:1812.06959 (2018), arXiv:1812.06959 [cond-mat.quant-gas].
- ¹⁹ K. X. Wei, C. Ramanathan, and P. Cappellaro, *Phys. Rev. Lett.* **120**, 070501 (2018).
- ²⁰ J. Smith, A. Lee, P. Richerme, B. Neyenhuis, P. W. Hess, P. Hauke, M. Heyl, D. A. Huse, and C. Monroe, *Nat. Phys.* [advance online publication](#) (2016).
- ²¹ G. Kucsko, S. Choi, J. Choi, P. C. Maurer, H. Zhou, R. Landig, H. Sumiya, S. Onoda, J. Isoya, F. Jelezko, E. Demler, N. Y. Yao, and M. D. Lukin, *Phys. Rev. Lett.* **121**, 023601 (2018).
- ²² M. Ovadia, D. Kalok, I. Tamir, S. Mitra, B. Sacépé, and D. Shahar, *Sci. Rep.* **5**, 13503 EP (2015).
- ²³ S. Bera, G. De Tomasi, F. Weiner, and F. Evers, *Phys. Rev. Lett.* **118**, 196801 (2017).
- ²⁴ In addition to achieving sufficiently large system sizes and long observation times other difficulties arise; we list two prominent examples: (i) Computations carry nonphysical numerical parameters that need to be converged, such as the bond dimension and time increments. Convergence can be difficult to achieve and will, in general, be sensitive to the calculated observable and the physical parameter regime. (ii) Quenches may produce transients or even asymptotic time traces that reflect properties of the initializing wavefunction rather than the thermodynamic equilibrium. In this case the results of studies using different initialization, e.g. random versus staggered states, may be difficult to compare. For example, Luitz et al.⁶¹ report values for the imbalance exponent ζ that are smaller than the values detected by Doggen et al.⁶² by a factor of two or more, e.g., near $W=2$. Both works claim convergence with respect to numerical parameters, while they differ in the choice of the initial state: random⁶¹ versus Néel⁶².
- ²⁵ R. Vosk, D. A. Huse, and E. Altman, *Phys. Rev. X* **5**, 031032 (2015).
- ²⁶ A. C. Potter, R. Vasseur, and S. A. Parameswaran, *Phys. Rev. X* **5**, 031033 (2015).
- ²⁷ K. Agarwal, E. Altman, E. Demler, S. Gopalakrishnan, D. A. Huse, and M. Knap, *Ann. Phys. (Berlin)* **529**, 1600326 (2017).
- ²⁸ D. J. Luitz and Y. B. Lev, *Ann. Phys. (Berlin)* **529**, 1600350 (2017).
- ²⁹ P. Prelovek, M. Mierzejewski, O. Bariii, and J. Herbrych, *Ann. Phys. (Berlin)* **529**, 1600362 (2017).
- ³⁰ S. Iyer, V. Oganesyan, G. Refael, and D. A. Huse, *Phys. Rev. B* **87**, 134202 (2013).
- ³¹ M. Lee, T. R. Look, S. P. Lim, and D. N. Sheng, *Phys. Rev. B* **96**, 075146 (2017).
- ³² V. Khemani, D. N. Sheng, and D. A. Huse, *Phys. Rev. Lett.* **119**, 075702 (2017).
- ³³ F. Setiawan, D.-L. Deng, and J. H. Pixley, *Phys. Rev. B* **96**, 104205 (2017).
- ³⁴ E. V. H. Doggen and A. D. Mirlin, arXiv e-prints, arXiv:1901.06971 (2019), arXiv:1901.06971 [cond-mat.dis-nn].
- ³⁵ We mention that the diffusion propagator has been studied before,^{28,29,63,64} but is not usually considered. Consequently, the exponent β has mostly been derived from closely related observables, such as (i) the frequency dependent conductivity at zero wavenumber calculated in finite size systems^{51,52,54,65,66} or (ii) the dynamical density response at wavenumber $q = \pi$ (imbalance)^{28,62}. Also the exponent of the return probability, α , has been employed, although the relation to β involves an extra exponent, which is not known with good accuracy²³.
- ³⁶ We include $\hat{\beta}(t)$ as an indicator with the idea that t_ξ is the only relevant time scale. Correspondingly, at $t \gtrsim t_\xi$ the sign of β is converged, while its numerical value may not be, yet.
- ³⁷ P. T. Dumitrescu, A. Goremykina, S. A. Parameswaran, M. Serbyn, and R. Vasseur, *Phys. Rev. B* **99**, 094205 (2019).
- ³⁸ Y. B. Lev, D. M. Kennes, C. Klöckner, D. R. Reichman, and C. Karrasch, *EPL (Europhysics Letters)* **119**, 37003 (2017).
- ³⁹ J. T. Chayes, L. Chayes, D. S. Fisher, and T. Spencer, *Phys. Rev. Lett.* **57**, 2999 (1986).
- ⁴⁰ When working with quasi-periodic potential (Aubry-André model) we choose, $\epsilon_x = W \cos(2\pi\alpha x + \phi)$ with $\alpha = 2/(\sqrt{5} + 1)$ and ϕ is the random phase distributed uniformly between $[0, 2\pi]$.
- ⁴¹ Here, we have used that in the infinite temperature limit the density is homogeneous and equal to $1/2$.
- ⁴² A. Weiße, G. Wellein, A. Alvermann, and H. Fehske, *Rev. Mod. Phys.* **78**, 275 (2006).
- ⁴³ Alternative possibilities could be (i) $b_1(W_{c_1})=0$ or (ii) $b_1(W_{c_1}) \rightarrow \infty$. The case (i) can be discussed when assuming the simplest possibility, which is that $b_1(W)$ crosses zero at W_{c_1} . In this case, the sign change associated with the crossing would imply according to (5) that transport continues to be subdiffusive once b_1 has changed sign; the effective diffusion exponent $\beta(t)$ then would be decreasing in time. This behaviour is not inconsistent with the numerical data, see Fig. 3, e.g., at $W=5$. Nevertheless, we do not follow this direction, here. Namely, a regime in disor-

der with $b_1(W)$ negative implies within the framework of (5) the possibility a pole at a finite value of ξ , which can be avoided only by assuming a kind of parametrical fine-tuning. The case (ii) is readily ruled out. It implies that at the transition $\dot{\beta}=0$ and $\beta=0$ vanish simultaneously. Also this behaviour is not consistent with the data Fig. 3.

- 44 V. Khemani, S. P. Lim, D. N. Sheng, and D. A. Huse, *Phys. Rev. X* **7**, 021013 (2017).
- 45 J. Gray, S. Bose, and A. Bayat, *Phys. Rev. B* **97**, 201105 (2018).
- 46 Z. Lenarčič, E. Altman, and A. Rosch, *Phys. Rev. Lett.* **121**, 267603 (2018).
- 47 A. Goremykina, R. Vasseur, and M. Serbyn, *Phys. Rev. Lett.* **122**, 040601 (2019).
- 48 L. Zhang, B. Zhao, T. Devakul, and D. A. Huse, *Phys. Rev. B* **93**, 224201 (2016).
- 49 T. Thiery, F. Huveneers, M. Müller, and W. De Roeck, *Phys. Rev. Lett.* **121**, 140601 (2018).
- 50 L. Herviou, S. Bera, and J. H. Bardarson, arXiv e-prints, arXiv:1811.01925 (2018), arXiv:1811.01925 [cond-mat.dism].
- 51 S. Gopalakrishnan, M. Müller, V. Khemani, M. Knap, E. Demler, and D. A. Huse, *Phys. Rev. B* **92**, 104202 (2015).
- 52 R. Steinigeweg, J. Herbrych, F. Pollmann, and W. Brenig, *Phys. Rev. B* **94**, 180401 (2016).
- 53 P. Prelovšek and J. Herbrych, *Phys. Rev. B* **96**, 035130 (2017).
- 54 O. S. Barišić, J. Kokalj, I. Balog, and P. Prelovšek, *Phys. Rev. B* **94**, 045126 (2016).
- 55 M. Mierzejewski, J. Herbrych, and P. Prelovšek, *Phys. Rev. B* **94**, 224207 (2016).
- 56 Y. Y. Atas and E. Bogomolny, *Philos. Trans. Royal Soc. A* **372**, 20120520 (2014).
- 57 I. V. Gornyi, A. D. Mirlin, D. G. Polyakov, and A. L. Burin, *Annalen der Physik* **529**, 1600360 (2017).
- 58 N. Macé, F. Alet, and N. Laflorencie, arXiv e-prints, arXiv:1812.10283 (2018), arXiv:1812.10283 [cond-mat.dism].
- 59 M. Serbyn, Z. Papić, and D. A. Abanin, *Phys. Rev. Lett.* **111**, 127201 (2013).
- 60 D. A. Huse, R. Nandkishore, and V. Oganesyan, *Phys. Rev. B* **90**, 174202 (2014).
- 61 D. J. Luitz, N. Laflorencie, and F. Alet, *Phys. Rev. B* **93**, 060201 (2016).
- 62 E. V. H. Doggen, F. Schindler, K. S. Tikhonov, A. D. Mirlin, T. Neupert, D. G. Polyakov, and I. V. Gornyi, *Phys. Rev. B* **98**, 174202 (2018).
- 63 Y. Bar Lev, G. Cohen, and D. R. Reichman, *Phys. Rev. Lett.* **114**, 100601 (2015).
- 64 Y. B. Lev and D. R. Reichman, *EPL (Europhysics Letters)* **113**, 46001 (2016).
- 65 K. Agarwal, S. Gopalakrishnan, M. Knap, M. Müller, and E. Demler, *Phys. Rev. Lett.* **114**, 160401 (2015).
- 66 I. Khait, S. Gazit, N. Y. Yao, and A. Auerbach, *Phys. Rev. B* **93**, 224205 (2016).
- 67 C. L. Bertrand and A. M. García-García, *Phys. Rev. B* **94**, 144201 (2016).

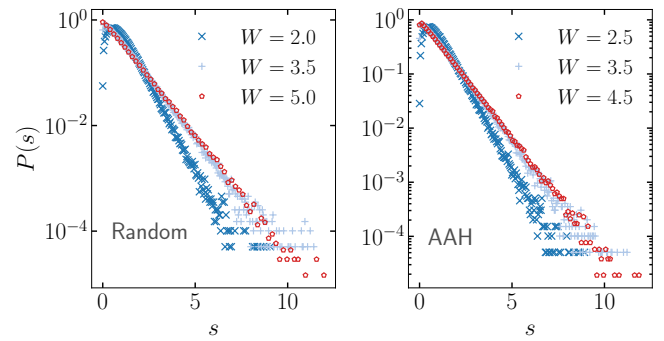


FIG. S1. Level spacing distribution for the $t-V$ -model at interaction strength $V=2t_h$ for the fully disordered model (left, $W/t_h=2.0, 3.5, 5.0$) and quasi-periodic (AAH) model (right, $W/t_h=2.5, 3.5, 4.5$) at system size $L=16$. Both panels show an evolution of the distribution from Wigner distribution towards Poisson statistics with increasing disorder.

Appendix A: Spectral statistics

Figure S1 shows the evolution of the level spacing distribution $P(s)$ for both the random and AAH model from weak (Wigner-Dyson statistics) to strong (Poisson distribution) disorder. The data is qualitatively similar to the one presented in Ref. 67. This illustrates that in a spectral sense the system is close to or even in the many-body localized phase for the disorder strengths that has been used in the main text (see Fig. 2).

Appendix B: Time dependence of $\Phi(x, t)$

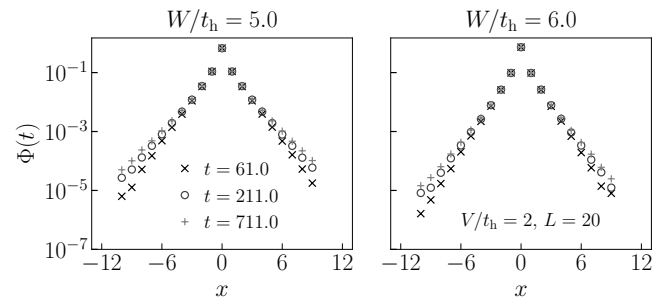


FIG. S2. Time evolution of the full distribution function $\Phi(x, t)$ for the random model at strong disorder. The slow dynamics manifests as tails lifting away from the nearly exponential shape that is indicative of the short time behavior and the non-interacting limit. The data is shown for $L=20$, $V/t_h=2$ and two different disorder values $W/t_h=5.0, 6.0$.

In the localized phase $\Delta x(t)$ increases slowly (as shown in Fig. 2) with time above the non-interacting saturation within our observation time ($\sim 10^3$ in unit of inverse t_h). In the distribution function $\Phi(x, t)$ this propagation is reflected via the lifting of the tails with time as seen in

Fig. S2. The tail-lifting eventually produces a stretched-exponential shape of $\Phi(x, t)$.

Appendix C: Oscillations in β

We analyze the spike observed in $\beta(\Delta x)$ (see Fig. 3), which becomes more pronounced at increasing disorder strength W . It occurs at $\Delta x \lesssim 1$ (cf. Fig. S3), and therefore we interpret it as a signature of the lattice spacing, which is taken as the unit of length. In essence, the spike is a manifestation of strong oscillations that induce a non-monotonous growth of $\Delta x(t)$ in time. Such oscillatory behaviour arises from neighboring pairs of sites that have a common local potential, which deviates strongly from the environment and thus is forming a "trap". The trap constitutes a two-site system with an associate energy doublet that is split by the hopping term. The dynamics of the associated charge density exhibits a characteristic frequency $\omega \approx t_h = 1$.

The corresponding oscillations in the correlator $\Phi(x, t)$ are illustrated in Fig. S3 for a given disorder configuration with trap near $x=0$. Strong oscillations are also seen in Fig. S5 differing from S4 by rescaling the on-site potential to smaller values with factor $3/5$ (blue) and $1.5/5$ (red).

We discuss the effect of interactions on time-dependent fluctuations in $\Delta x(t)$: In the non-interacting limit, $V=0$, pronounced oscillations are seen large disorder (corresponding to strength $W=2$) in S4; they persist up to very long times. With decreasing disorder, Fig. S5, lower frequencies are typically mixing in because resonances between more distant sites become accessible, converting oscillations to mesoscopic fluctuations. This type of oscillation survives the ensemble average, because return times tend to be integer multiples of $2\pi/t_h$.

With finite interaction the random potential will, in general, undergo a static renormalization; it shifts fluctuation frequencies without affecting the qualitative

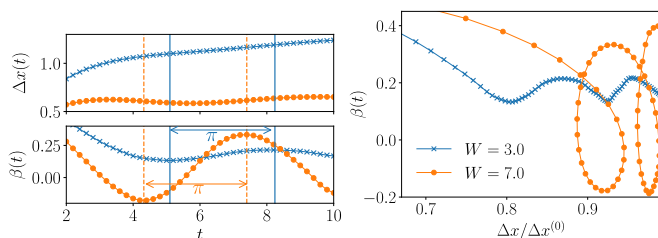


FIG. S3. Short-time behavior of $\Delta x(t)$ and $\beta(t)$ averaged over several thousand samples. Figure is illustrating the origin of the peak-structure seen in Fig. 3 of the main text at intermediate (blue) and strong (orange) disorder: $W=3.0, 7.0$. Left: $\Delta x(t)$ exhibits oscillatory behaviour that is emphasised in its logarithmic derivative, $\beta(t)$. At strong enough disorder, $W > W^*$, $\Delta x(t)$ becomes non-monotonous. Vertical lines indicate a half-period of the oscillation. Right: Multivalued $\beta(\Delta x)$ at $W > W^*$.

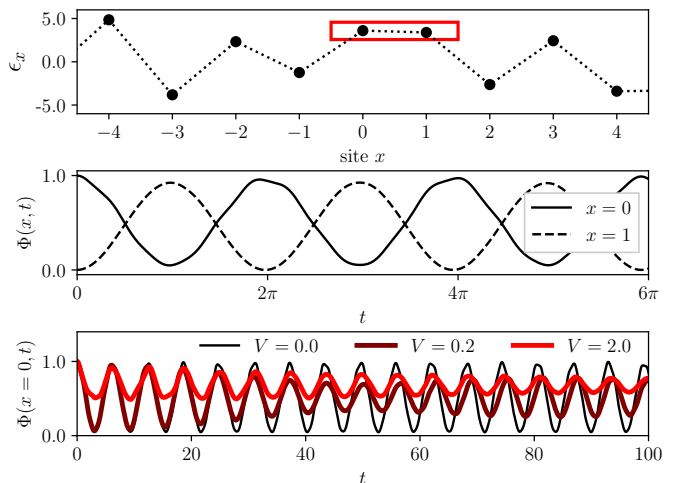


FIG. S4. Behavior of $\Phi(x, t)$ around $x = 0$ for a given disorder configuration. Note that $\Phi(x, t = 0) = \delta_{x,0}$, by definition. Top: Disorder potential ϵ_x around $x = 0$: sites $x = 0, 1$ are very close in energy. Center: Coherent oscillations between neighboring sites $x = 0, 1$ in the non-interacting limit $V = 0$. The period is close to 2π . Bottom: Damping for finite interaction strength V .

physics. New effects can be expected from dynamical renormalizations, i.e., from dephasing; it is a characteristic feature of many-body systems expressing the possibility of particles to scatter off each other and thus exchanging momentum and energy. In the correlator $\Phi(x, t)$ dephasing manifests itself in a damping of the mesoscopic fluctuations, see Fig. S4, bottom and S5. The defining characteristics of the mbl-phenomenon is that despite mesoscopic fluctuations washing out very quickly with increasing V , the average return probability is seen to keep values of order unity that hardly decay at all, see Fig. S4 and S5.

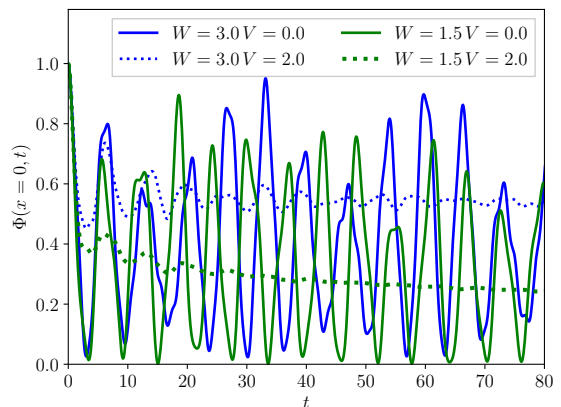


FIG. S5. $\Phi(x=0, t)$ for the same disorder configuration as in Fig. S4 but rescaled such that $\epsilon_x \in [-W, W]$. Oscillations become increasingly irregular with decreasing W .

Appendix D: Evolution of $\Delta x(t)$ in a quasi-periodic (AAH) potential

In the main text we have analysed the evolution of the correlator $\Phi(x, t)$ for the case of fully disordered potentials, Fig. 3. We here display the analogous data obtained for the quasi-periodic case.

Thermalizing regime. Before we discuss the main data set, Fig. S7, we report an effect that we observe for quasi-periodic potentials, which is not seen in the fully random case. In Fig. S6 we show the correlation function $\Phi(x, t)$ at very large times. Despite the fact that the dynamics has explored the full system size, oscillations are seen that do not show a tendency to equilibrate, see also Fig. S7 for other disorder values.

While a detailed study of this effect is beyond the scope of this work, a few comments are in place. A preliminary analysis suggests that the amplitude of the oscillations decays with increasing system size in a power law-fashion; therefore, we tentatively consider them as a finite size effect. Presumably, the oscillations are related to the correlations in the underlying quasi-periodic potential; hence, one would expect that their shape is sensitive to the choice of the parameter α in the definition of ϵ_x (see 40 for further details). Furthermore our data Fig. S7 indicates that due to these oscillations at moderate disorder $W=1.5 - 3.0$, i.e. in a regime that is believed to be thermal, finite size effects can be strong. We believe that they should be observable, in principle, also in typical cold-atom experiments¹⁵. Finally, in recent computational work it was found that the critical disorder strength could also be dependent on α : $W_c(\alpha)$ ³⁴. Conceivably, this finding is related to effects such as displayed in Fig. S6.

The analysis of $\Phi(x, t)$ for the quasi-periodic case in terms of the effective exponent $\beta(t)$ is done in analogy to the fully random case. The middle panel of Fig. S7 displays the evolution of $\Delta x(t)$ at system sizes

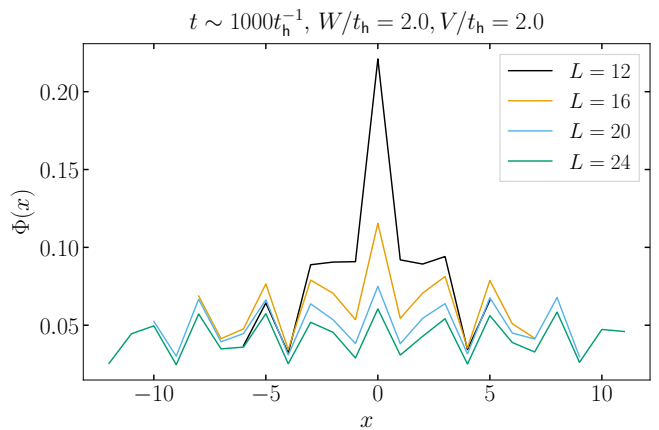


FIG. S6. $\Phi(x, t)$ at moderate strength of the quasi-periodic potential displayed at a very large observation time $t \sim 10^3 t_h^{-1}$ for system sizes $L=12, 16, 20, 24$.

$L=12, 16, 20, 24$ for interaction $V/t_h = 2.0$. At small disorder, $\Delta x(t)$ is seen to reach a plateau value $\approx L/3.5$ indicating saturation due to the finite system size. While the saturation width is only slowly decreasing with disorder, W , the saturation time is clearly seen to be a strongly growing function of W exceeding the computational time window already at moderate disorder $W=2.5$.

Lower panel shows the corresponding evolution of the logarithmic derivative of $\Delta x(t)$, i.e. the exponent function $\beta(t)$. As announced before, the evolution for the quasi-periodic case is analogous to the random disorder case (see Fig. 3 lower panel). In particular, extremely strong finite size effects hamper a reliable extraction of the asymptotic exponent. The overall trend is that the short-time exponent at weak disorder takes larger values which are not far from the diffusive regime, $\beta=1/2$.

Strong disorder. At stronger disorder the level statistics is seen to approach the Poissonian limit in (Fig. S4). We thus associate with disorder values $W \gtrsim 5$ a regime close or in the many-body localized phase. Correspondingly, with increasing disorder the dynamics as displayed by $\Delta x(t)$ slows down considerably, see Fig. S8; in the quasi-periodic and the fully random situations it shows the same qualitative behavior. Since effects of rare regions are not expected in the quasi-periodic situation, our observations suggest that the typical strong disorder effects may not be the origin of slow dynamics and creep.

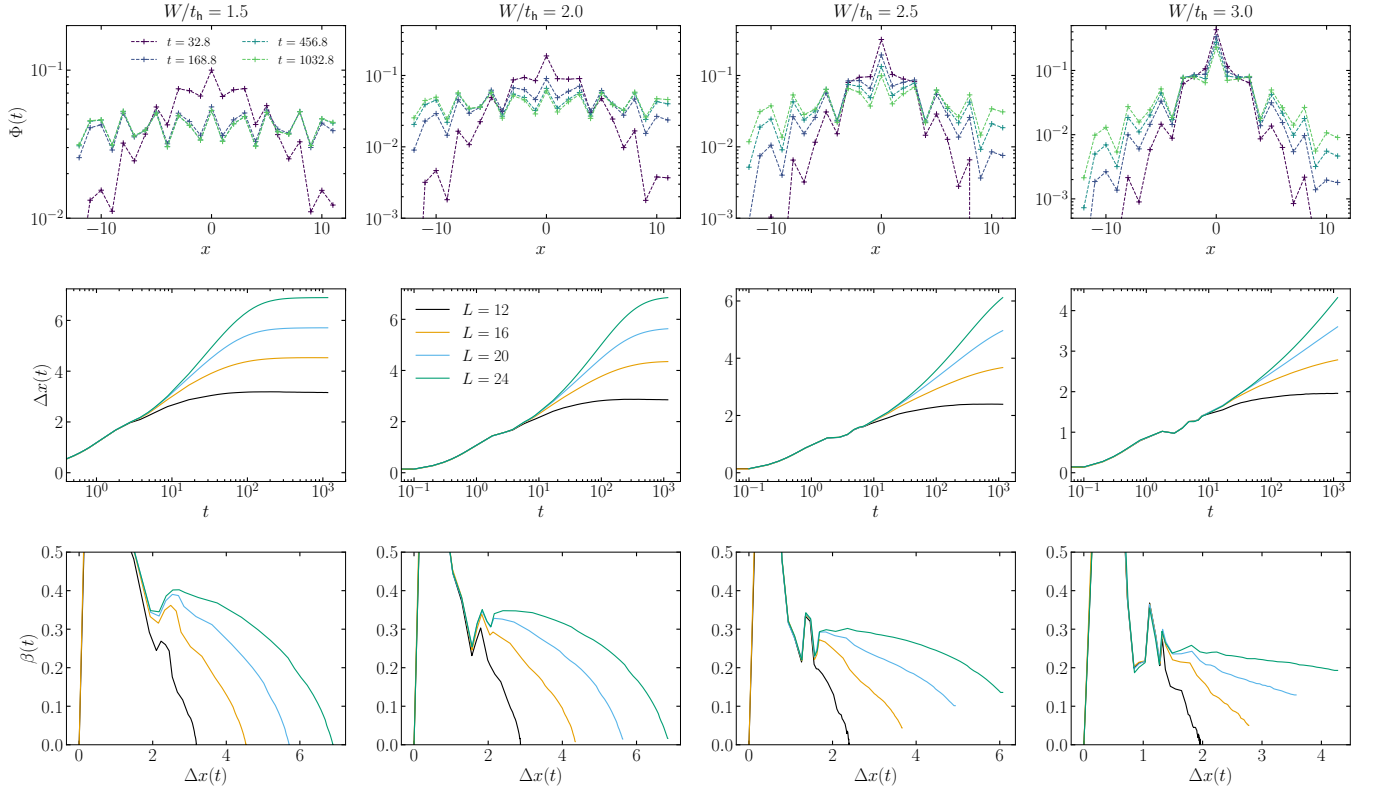


FIG. S7. Upper panel: Shows the evolution of $\Phi(t)$ for different values of disorder ($W/t_h = 1.5, 2.0, 2.5, 3.0$) at interaction $V/t_h = 2.0$ for the AAH model for $L = 24$. Inset (b) displays the long time density correlator that shows pronounce oscillation, which is reminiscent of the underlying quasi-periodic potential (black dashed line). Middle row shows the corresponding $\Delta x(t)$ and the lower panel displays the evolution of $\beta(t)$ with system sizes ($L = 12, 16, 20, 24$) for different disorder values.

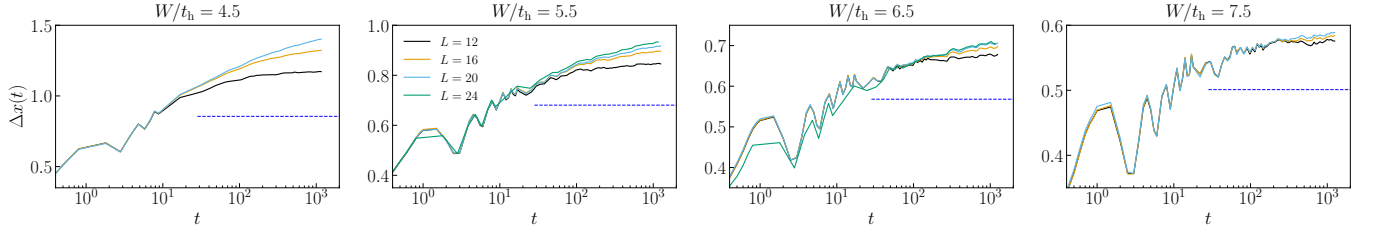


FIG. S8. Shows the time evolution of $\Delta x(t)$ for different values of disorder strength $W/t_h = 4.5, 5.5, 6.5, 7.5$ and for interaction strength $V/t_h = 2.0$. The dashed line (blue) is indicating the non-interacting value of $\Delta x(t)$ for corresponding disorder strengths for $L = 16$ obtained from separate computations.